# Application of spectral quantization to metastable states of $C\ ^1A'$ DCN

David T. Chuljian,[a] Judy Ozment,[b] and Jack Simons
*Department of Chemistry, University of Utah, Salt Lake City, Utah 84112*

(Received 4 March 1986; accepted 12 August 1986)

The spectral quantization method which was successfully used previously to study bound state energies and wave functions of $C\ ^1A'$ DCN is extended to the low-lying metastable states of this same system. The potential energy surface employed involves the same *ab initio* calculational data as was used in our earlier classical trajectory and purely quantal studies. Energies and wave functions for the metastable states of DCN obtained by spectral quantization are compared to those achieved in the presumably accurate quantal study. The agreement between the quantal and spectal quantized wave function is not nearly as pleasing for these metastable states as it was for the bound states.

## I. INTRODUCTION

Systems undergoing unimolecular decomposition are currently the object of much theoretical and experimental study. Many of the experimentally interesting systems, however, are too complex to be studied theoretically using rigorous quantum methods; thus there has been much emphasis in recent years on developing and testing approximate methods for studying the internal (vibrational) motion of unstable molecules. In particular, quasiclassical trajectory (QCT) methods have been used to study both unimolecular decomposition[1] and reactive scattering,[2] and the resultant classical predictions, whenever possible, have been compared with rigorous quantal results. Because there are situations for which a purely classical approach is inappropriate, various semiclassical methods have been proposed,[3,4] and tested on model systems. In early semiclassical studies, the major emphasis was on determining the energy levels for the bound states of the systems. More recently, however, there has been interest in calculating the semiclassical wave functions as well.[5]

In a recent series of papers, we have studied by both quantal and semiclassical methods the predissociation dynamics of the $C$ state ($^1A'$) DCN molecule.[6,7] Experimentally,[8] this system shows vibrational predissociative behavior, with the vibrational state lifetimes being strongly dependent on the values of the D–CN stretching and bending quantum numbers ($v_1$ and $v_2$, respectively). In Ref. 6, which we hereafter refer to as paper I, we developed a model (with the CN bond length frozen) for $C$ state DCN predissociation, and calculated fully quantal energies and wave functions for the bound and metastable states of this model; the quantal lifetimes were compared with QCT lifetimes and with stabilization based results. (For a description of the method used in the quantal studies, and detailed results, the reader should consult paper I.) In a subsequent study,[7] which we hereafter refer to as paper II, semiclassical wave functions for the bound states of this model system were generated using a method closely related to the spectral quantization (SQ) method of De Leon and Heller.[9] The SQ method allows one to obtain both the energy levels and the wave functions for a given molecular Hamiltonian using a single classical trajectory; the classical action of the trajectory may or may not be required to be quantized. In paper II, the SQ wave functions for the bound vibrational states of the $C$ state DCN model system were compared with the corresponding quantal wave functions, and good to excellent agreement was obtained. The $C$ state electronic potential surface of DCN is a strongly anharmonic surface, with the bending and stretching modes highly coupled, hence we were gratified to note that the SQ method so quantitatively reproduced the quantum wave functions for this realistic molecular model. Equally encouraging was the fact that the quantal/SQ agreement held for a wide range of energies: from the ground vibrational state, up to states near the dissociation threshold. For these higher vibrational states, the D atom samples regions of the potential surface which are highly mode coupled and very anharmonic.

The SQ method, and its modifications, had not previously been tested for such a challenging potential energy surface, and the success noted in the studies of paper II encouraged us to apply SQ to the metastable states (resonances) of the same model problem. We realized that the resonance states presented a much greater challenge to the SQ method than did the bound states. However, as a first approximation to the resonance vibrational states, one expects (or at least hopes) them to be extrapolations of the bound states: that is, reasonably localized, showing fairly simple nodal patterns, and with energy level spacings similar to the spacings of the higher energy bound spectrum. In fact, the quantal resonance states of our model of DCN *did* display such regularity in their energy levels and nodal patterns,[6] which encouraged us to extend the SQ method to above threshold. Although paper II showed a gradual deterioration in the SQ/quantal agreement at higher (bound) energies, it still seemed reasonable to expect SQ to give good qualitative information about the resonance state wave functions and dissociation dynamics.

In the remainder of this paper, we compare SQ wave functions for the metastable states of our model system with the earlier quantum mechanical results. Section II describes how we applied the SQ method to the metastable states of our model, briefly reviews the quantal results, and summarizes the dissociation dynamics of $C$ state DCN. Section III gives state-by-state comparisons of the SQ and quantal wave

[a] Present address: 415 Fillmore St., Port Townsend, WA 98368.
[b] Present address: Department of Chemistry, University of Washington, Seattle, WA 98195.

 0021-9606/86/225826-12$02.10 

functions where we observe that the SQ and fully quantal eigenfunctions are not nearly in as good agreement as for the bound states. Section IV investigates the causes of the SQ/quantal discrepancies, and discusses the capabilities of the SQ method in the study of resonances. In Sec. V, we discuss the outlook for the SQ method, and other semiclassical wave packet methods, in the study of metastable states.

## II. HOW DID WE STUDY THESE METASTABLE STATES?

### A. Spectral quantization study of resonances

The SQ method is described in paper II and references therein, hence we will only briefly summarize the procedure here. The essence of the method is the propagation of a Gaussian wave packet along a classical trajectory. A time-evolving wave packet, if propagated fully quantum mechanically, would contain components of the exact eigenstates of the system; by suitable projection, these exact eigenstates could be recovered.[5] The propagation of a *frozen* wave packet along a *classical* trajectory is the most crucial approximation in the SQ method.

For bound states, we apply the SQ method as follows. Given the molecular Hamiltonian, we propagate a classical trajectory having an energy near that of the state we wish to study until the trajectory closes on itself (i.e., until all coordinates and momenta coincide with the initial coordinates and momenta to within some small tolerance).[10] A Gaussian "coherent state wave packet" (CSW) is then constructed and propagated in time *along* the trajectory.[5,9] The CSW is "frozen"; that is, it is assumed not to spread or otherwise distort as it propagates (in fact, for a globally harmonic potential surface, this assumption is exactly satisfied if the surface's harmonic frequency matches that of the packet).[11] A Fourier energy transform of the overlap of the propagated CSW with the CSW at $t=0$ then gives a power spectrum, the peaks of which, $\{E_i\}$, are the semiclassical eigenvalues.[7,9] The projection of the desired eigenstate $\psi_J$ is then carried out by repropagating the CSW with its phase modified by $\exp(iE_jt/\hbar)$; this usually works best if there is a large peak in the power spectrum corresponding to the desired eigenstate's energy $E_j$. As the phase-shifted wave packet propagates along the original trajectory, amplitude is built up and destroyed, depending on the relative phase of the propagated wave packet. This constructive and destructive interference pattern gives the SQ estimate for the eigenfunction.

Our approach to the SQ study of metastable states is very similar to that described above; indeed, we use some of the same bound trajectories. It was noted in paper II that the power spectra of the higher energy bound trajectories contained peaks corresponding to energies above the dissociation threshold; in some cases, these were the *largest* peaks.[12] This would imply that SQ wave functions for the metastable states were the major components of these high energy (but still bound) wave packets. Accordingly, for each resonance we propagated a CSW along a high energy bound trajectory, with the phase modified by the factor $\exp(iE_jt/\hbar)$ corresponding to the power spectrum peak $E_j$ associated with the energy (position) of the resonance, and thus obtained the SQ estimate for the resonance wave function.

One may reasonably ask, why not look for closed trajectories with energies above threshold? Unfortunately, the vast majority of trajectories above threshold eventually dissociate rather than close. The few closed trajectories we did find above threshold represented rather specialized motion (i.e., they sampled a very small fraction of the accessible phase space); such trajectories are not appropriate for producing wave functions, since they do not contain information about the wave function amplitude within most of the energy-allowed potential surface. A further justification for the use of high energy bound trajectories is that the bound state SQ wave functions of paper II were seen to depend only weakly on the particular trajectory used. As long as the classical trajectory sampled most of the energy-allowed phase space, displaying motion of the type expected for the particular quantum state, and was reasonably close to the energy of the desired state (within about 1000 $cm^{-1}$), the results were quite similar. Thus the most promising trajectories for studying metastable states seemed to be those which: (i) had energies close to threshold and (ii) fairly uniformly sampled the allowed phase space. Several such trajectories (with varying amounts of stretching and bending motion) were used in order to obtain power spectra with major peaks corresponding to the several different metastable states in the energy range of interest (100–1000 $cm^1$ above threshold).

### B. Quantal studies: Resonance energies and lifetimes

The bound and metastable states of our model of $C$ state DCN were studied using the method of complex scaling of the Hamiltonian, sometimes referred to as "coordinate rotation" (CR).[6,13] In the CR method, one scales the dissociative coordinate (denoted $r$) by a complex parameter $\eta = \alpha e^{i\theta}$, and forms the "rotated" Hamiltonian,

$$H(r) \rightarrow H_\eta = H(\eta r). \tag{1}$$

The bound states of the Hamiltonian are invariant to $\eta$. For $\theta$ larger than a critical value $\theta_c$, metastable states of the rotated Hamiltonian behave like bound states of a typical Hamiltonian; that is, their energies are stationary with respect to changes in the variational parameters, and their wave functions are square integrable. The latter property permits the study of the resonances by expansion in standard bound-state basis sets. The complex energy of a resonance is stable with respect to changes in $\theta$ for $\theta > \theta_c$ and is written as

$$E = E_{\rm res} - i\Gamma/2. \tag{2}$$

Here, $E_{\rm res}$ is the position of the resonance; $\Gamma$ is the width of the resonance, and is related to the lifetime by

$$\tau = \hbar/\Gamma. \tag{3}$$

A more detailed discussion of the CR method is out of place here, and the reader is referred to several excellent reviews on the subject.[13,14] In this paper, we treat CR as an established method capable of giving accurate results for the resonances of our model.[15] Our CR estimates for the resonance positions and widths are listed in Table I.[16]

As noted in paper I, our radial basis is only adequate to accurately represent resonances in the energy range of 150–1000 $cm^{-1}$; thus the $(v_1=1, v_2=3)$ resonance lying about 100 $cm^{-1}$ above threshold is not as well described as the

TABLE I. CR estimates for the resonance positions and widths.

| $(v_1,v_2)$ | $E_{res}$[a] | $\Gamma$[a] | $\tau_{CR}$[b] | $\tau_{QCT}$ (%)[c] |
|---|---|---|---|---|
| (4,0) | $-20$[d] | 0 | $\infty$ | $\cdots$ [$\cdots$][e] |
| (1,3) | $<100$[f] | 10–20[f] | 0.35[f] | 0.52 [ 90] |
| (0,6) | 220–225 | 5–10 | 0.71 | 0.85 [100] |
| (3,1) | 350[g] | $>100$[h] | $<0.05$[h] | 0.35 [ 34] |
| (2,2) | 380–390 | 15–20 | 0.30 | 0.14 [ 55] |
| (1,4) | 680–690 | 20–40 | 0.18 | 0.18 [ 89] |
| (0,7) | 860–870 | 20–25 | 0.24 | 0.21 [100] |
| (3,2) | 950[g] | $>100$[h] | $<0.05$[h] | 0.14 [ 32] |

[a] From CR calculations, $E = E_{res} - i\Gamma/2$; energy in $cm^{-1}$.
[b] $\tau_{CR} = \hbar/\Gamma$; units of ps ($10^{-12}$ s).
[c] $\tau$ as calculated by slow-channel QCT method (see the Appendix); (value) is the percentage of slow-channel trajectories.
[d] The state (4,0) is bound, according to the CR calculations; hence $\Gamma$ is zero and the state's lifetime is infinite.
[e] No QCT calculations were carried out for the (4,0) state.
[f] A range of energies is reported to indicate the approximate computational uncertainties; the value reported for $\tau_{CR}$ is obtained using the mean value of $\Gamma$.
[g] No resonance was located by CR calculations (see the text); the position given is from extrapolation of the bound state energy spacings.
[h] Lower bound for the width and upper bound for the lifetime, based on capabilities of the basis (see the text).

other resonances. We also note that as $\theta$ is increased beyond $\theta_c$, the resonance wave functions (in contrast to the resonance energies) *do* change; oscillations develop in their radial-coordinate dependence.[17] Our square-integrable radial basis cannot describe very rapid oscillations, and is inadequate for $\Theta$ greater than about 0.030 rad. According to the original CR theorems, this restriction to small $\theta$ means that very broad resonances cannot be described by our basis. A rough estimate is that resonances with lifetimes of less than 0.05 ps ($10^{-12}$ s) will be indistinguishable from continuum states.

We were unable to locate a resonance for ($v_1 = 3$, $v_2 = 1$) in the CR calculations, and we thus assume that this state's lifetime is less than 0.05 ps. It is possible that some defect in our basis caused us to grossly underestimate the lifetime of the (3,1) state, but this seems unlikely inasmuch as the states (3,0), (4,0), and (2,2) were adequately described by the basis. The (3,2) state is presumably even more shortlived than the (3,1) state, hence we did not attempt to locate the (3,2) resonance.

### C. The quantal dynamics of *C* state predissociation

We conclude Sec. II by examining the predissociation dynamics of *C* state DCN. Our two-dimensional potential energy surface is shown in Fig. 1; Fig. 2 shows a plot of the localized component of the wave function amplitude for the state ($v_1 = 0$, $v_2 = 6$), which is a typical narrow resonance. The plot has been scaled to show the large $r$ behavior, thus the peaks of the small $r$ part of the wave function have been "chopped off," but one can easily see the characteristic high-bending-state nodal pattern—seven peaks arranged in an arc. Note the low wave function amplitude at large $r$ in regions of the potential surface which possess barriers; that is, some tunneling behavior may be occurring, but not much. The majority of the large $r$ density is in the barrier-free region, and corresponds to classically allowed escape.

Close examination of the arc of peaks indicates that: (i) the peaks "bulge" out beyond the bottom of the potential well; (ii) near the endpoints of the arc, movement across a node (between peaks) actually involves D–CN stretching as well as bending motion—that is, there is coupling of the stretching ($v_1$) and bending ($v_2$) modes; and (iii) the highest amplitude peak is at linear geometry—$\theta = 180°$. (The other resonance wave functions are shown in Sec. III; the predissociation dynamics is qualitatively the same, although the extent of tunneling, mode coupling, etc., varies from state to state.)

As noted above, tunneling contributes only slightly to the predissociation. We do not expect tunneling to be at all well reproduced by SQ wave functions, since they are based on classical motion. The observed relative unimportance of

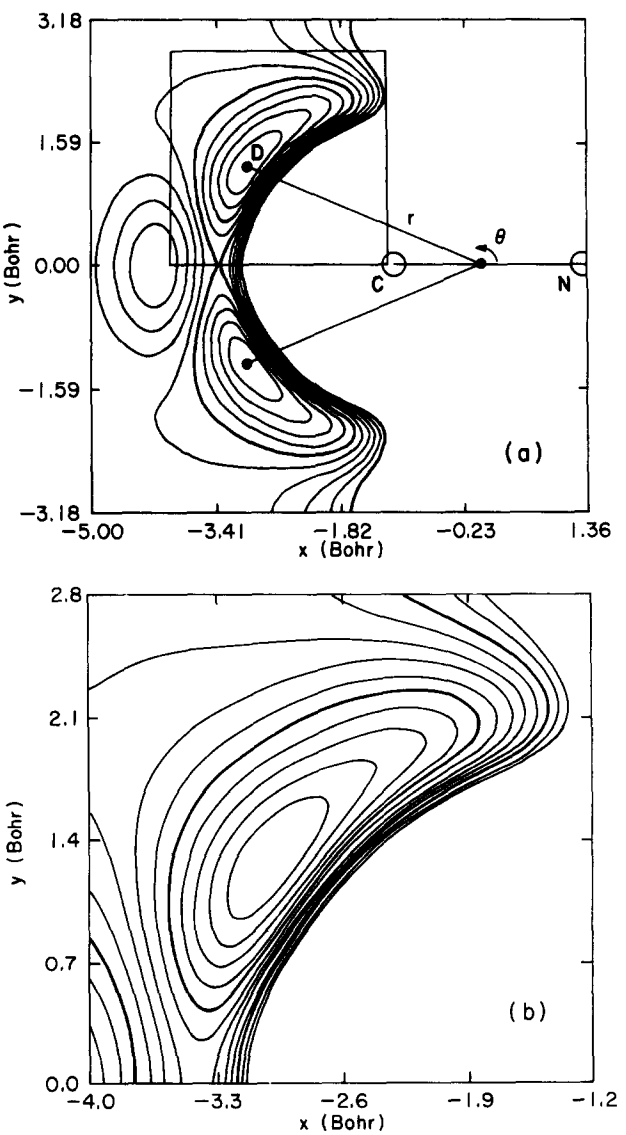


FIG. 1. (a) Potential energy surface of *C* state ($^1A'$) DCN; plane polar coordinates (r,Θ) shown. Each contour represents an increase of 0.0031 hartree; the minimum lies at r = 3.29 bohr and Θ = 157°, and the origin is the center of mass of the C–N bond. (The surface shown is $V_{poly}$; see Sec. IV A 1 and Fig. 5.) (b) Enlargement of the inset area of Fig. (1a); each contour represents 0.0023 hartree.

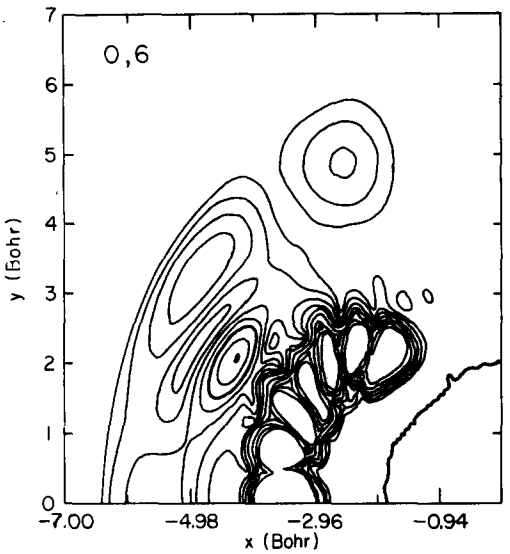


FIG. 2. Quantal wave function for the state ($v_1 = 0, v_2 = 6$). A larger area of the potential energy surface is shown than in Figs. 3 and 4, and the plot has been scaled to demonstrate the large $r$ behavior.

tunneling in the DCN predissociation dynamics makes this system more favorable for SQ studies. Intermode energy exchange is the dominant mechanism of predissociation; the degree of bend/stretch coupling primarily determines the decay rates (lifetimes) of the resonance states. Since our application of the SQ method is based on high energy trajectories which sample the coupled areas of the potential surface, it seems reasonable to expect SQ wave functions to show evidence of intermode coupling (i.e., bulge and bend/stretch distortion). Our implementation of SQ, of course, *cannot* be expected to show classical escape, since we use bound trajectories. We now examine some SQ wave functions for the metastable states, and compare them with the quantal wave functions.

## III. OVERVIEW OF THE QUANTAL/SEMICLASSICAL COMPARISON

In Figs. 3 and 4, contour plots of the resonance wave functions are shown for the SQ and quantal descriptions, respectively (also included are a few bound state wave functions for comparison). There are no quantal wave functions shown for the states (3,1) and (3,2) since no quantal resonances were located for those states. The positive quantity plotted in each case is the amplitude $A$ of the wave function written as

$$\Psi(r,\theta) = A(r,\theta)e^{i\phi(r,\theta)}. \tag{4}$$

Here $r$ is the distance from the D atom to the CN center of mass, and $\theta$ is the angle between $r$ and the CN bond axis; 180° corresponds to linear DCN. (For viewing convenience, all figures are labeled by $x$ and $y$, where $x = r\cos\theta, y = r\sin\theta$.) The lifetimes predicted by the QCT method[6,18] (described in the Appendix) are listed with the quantal lifetimes in Table I; for comparison, the bending and stretching periods of DCN are about 0.05 and 0.02 ps, respectively. The positions given for the resonances are the CR estimates; as implemented here, SQ does not give estimates for the positions (see paper II). The agreement is reasonable, except for the (3,1) and (3,2) states, for which the classical lifetimes are apparently much too long, judging from our failure to locate these states in our quantal studies. In calculations closely related to the QCT method used here, Moiseyev recently obtained resonance lifetimes which were a factor of 4–7 too long.[19] Bosanac has also cast doubt on the applicability of classical trajectory methods in predicting resonance state lifetimes.[20] Thus the good QCT/CR agreement for most of the lifetimes reported here may be fortuitous.

An analysis of the causes for the discrepancies between the quantal and SQ results will be given in Sec. IV; we merely note here the areas of agreement and disagreement. (i) The SQ resonance wave functions are qualitatively correct in the regions sampled by the trajectories. The nodal structure allows easy identification of the vibrational quantum numbers of the resonance states. (ii) The amount of distortion of the SQ wave functions does not agree well with that seen in the quantal wave functions. The SQ wave functions show nodal patterns which are too regular, and they do not bulge out beyond the potential well as much as do the quantal wave functions. (iii) The quantal wave functions show a pronounced density buildup near linear geometry ($y = 0$); the SQ wave functions show this to a lesser extent. (iv) The details of the predissociation dynamics are not very well reproduced by the SQ wave functions; as expected, the SQ wave functions do not infer tunneling (i.e., they do not show much density outside the classically allowed energy envelope). (v) Our inability to locate quantal resonances for the (3,1) and (3,2) states implies that the wave functions for these states should be very diffuse; however, well-localized SQ wave functions corresponding to large peaks in the power spectrum were obtained for these states.

## IV. DISCUSSION

As noted in Sec. III, there are a number of differences betwen the fully quantal and the SQ wave functions for the metastable states of $C$ state DCN. Here we address possible causes of these differences, and suggest modifications of the SQ method which should make it more suitable for the study of metastable systems.

### A. Causes of the SQ quantal wave function discrepancies

#### *1. Potential energy surface differences*

Before we compare the quantal and SQ wave functions, it is important to note that the potential energy surfaces used in the two studies, while very similar, were *not* the same surface. The quantal studies required that the potential surface be expressed in a particular form,[6]

$$V_{\text{num}}(r,\theta) = \sum_l V_l(r)P_l(\cos\theta), \tag{5}$$

where $P_l$ is the $l$th-order Legendre polynomial, and $V_l(r)$ was numerically determined to optimize the fit to $V_{\text{poly}}$ [see Eq. (6) below]. The SQ studies were based on earlier classical trajectory studies[1(a)] which used a polynomial fit to the

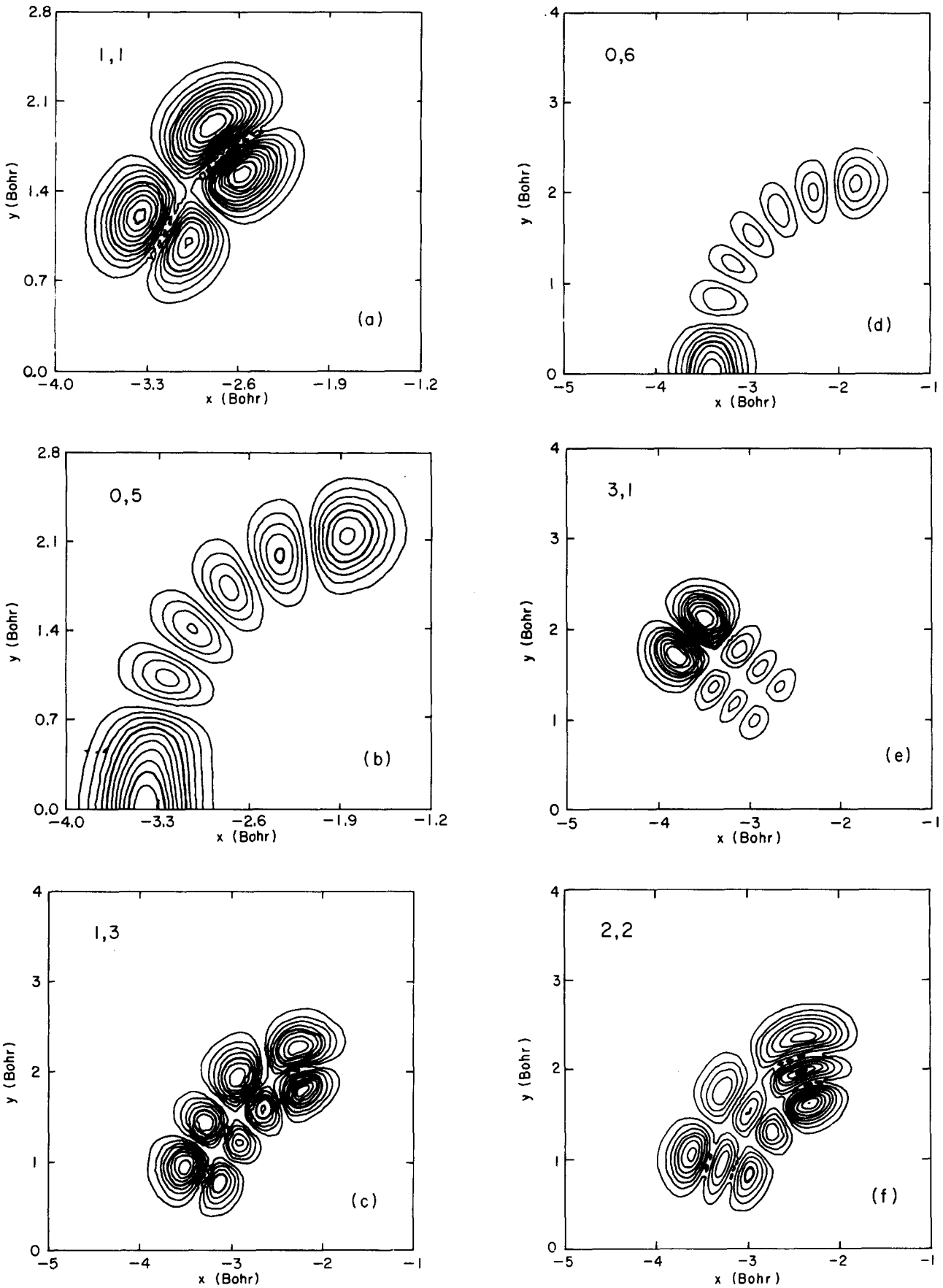


FIG. 3. Semiclassical (SQ) vibrational wave functions for $C$ state DCN; plotted as contour diagrams showing the magnitude $A$ of the wave functions [see Eq. (4)]. The contours are evenly spaced, but the division between contours is not the same in all the figures. (a) ($v_1 = 1, v_2 = 1$), a medium-energy bound state. (b) (0,5), a high-energy bound state. (c)–(i) are the SQ wave functions for the metastable states in order of increasing energy; the state labels ($v_1$,$v_2$) are shown in the upper left-hand corner. (A slightly larger area of the potential surface is shown for the metastable states than for the two bound states.)

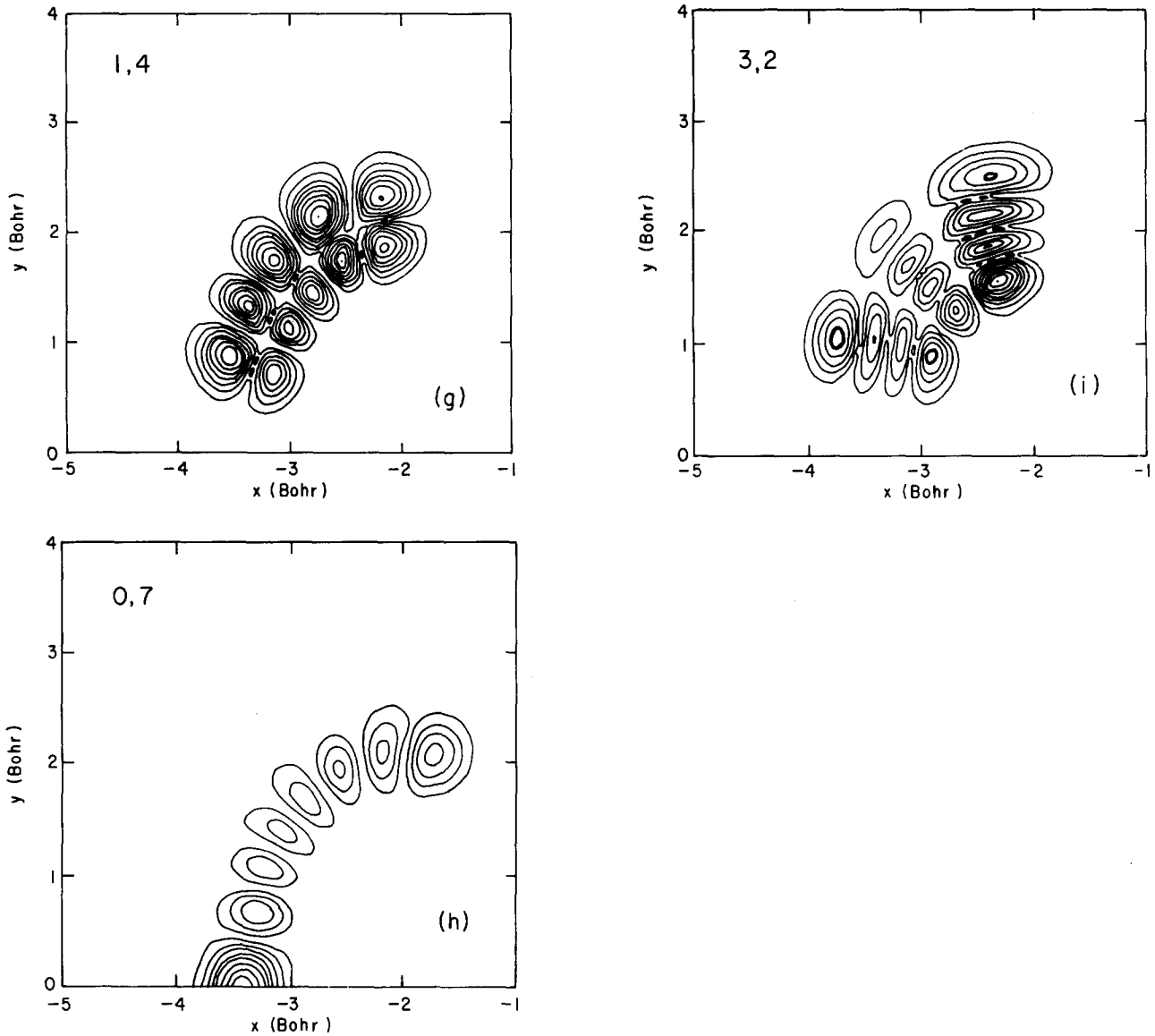


FIG. 3. (*continued.*)

*ab initio* potential surface,[21]

$$V_{\text{poly}}(r,\theta) = \sum_{m,n} C_{mn} r^m (\cos\theta)^n, \tag{6}$$

where $(m, n)$ are integer exponents, and the $C_{mn}$ are determined by a least squares procedure. $V_{\text{poly}}$ agreed to within about 40 $\text{cm}^{-1}$ with the *ab initio* energies[21] over a wide range of $(r,\theta)$, and was used for the SQ studies reported here except where specifically noted otherwise.

The two surfaces, $V_{\text{num}}$ and $V_{\text{poly}}$, are reproduced as contour plots in Figs. 5(a) and 5(b), respectively. They are seen to be very similar. However, it was noted that use of $V_{\text{num}}$ in the SQ computer routines led to a great increase in computer time, thus complicating the search for suitable closing trajectories. Test calculations were carried out, comparing SQ wave functions obtained using $V_{\text{num}}$, designated $\psi^{\text{SQ}}_{\text{num}}$, with those obtained using $V_{\text{poly}}$, $\psi^{\text{SQ}}_{\text{poly}}$. No significant differences were noted, and we concluded that it was appropriate to use $V_{\text{poly}}$ in further SQ wave function calculations.

Unfortunately, the above conclusion is far less valid for resonance wave functions, and even for high energy bound state wave functions. In Fig. 5 it is seen that the differences between the two surfaces occur in regions of the high energy contours. Because our early test calculations used relatively low energy trajectories, the significantly different parts of the surfaces did not contribute appreciably to the wave functions. Note that: (i) $V_{\text{num}}$ has a shallower, broader approach to the saddle point region at 180°; (ii) $V_{\text{num}}$ has a narrower escape path at the equilibrium angle of 157°; and (iii) the "side barriers" on $V_{\text{poly}}$ (at about $x = -2, y = \pm 3$) are smoother than those on $V_{\text{num}}$ (which suddenly get much steeper for $x > -1.5$). Dynamically, the first difference results in high energy trajectories on $V_{\text{num}}$ being much more prone to cross the saddle. This explains one of the discrepancies of Sec. III: the smaller wave function amplitude at 180° noted for the SQ wave functions is due to the fact that the classical trajectories which generate them do not cross the saddle. The lower distortion of $\psi^{\text{SQ}}_{\text{poly}}$ relative to the quantal wave functions $\psi^{\text{CR}}_{\text{num}}$ is not so easily explained, but it might be due to the different side barrier shapes of the two surfaces.

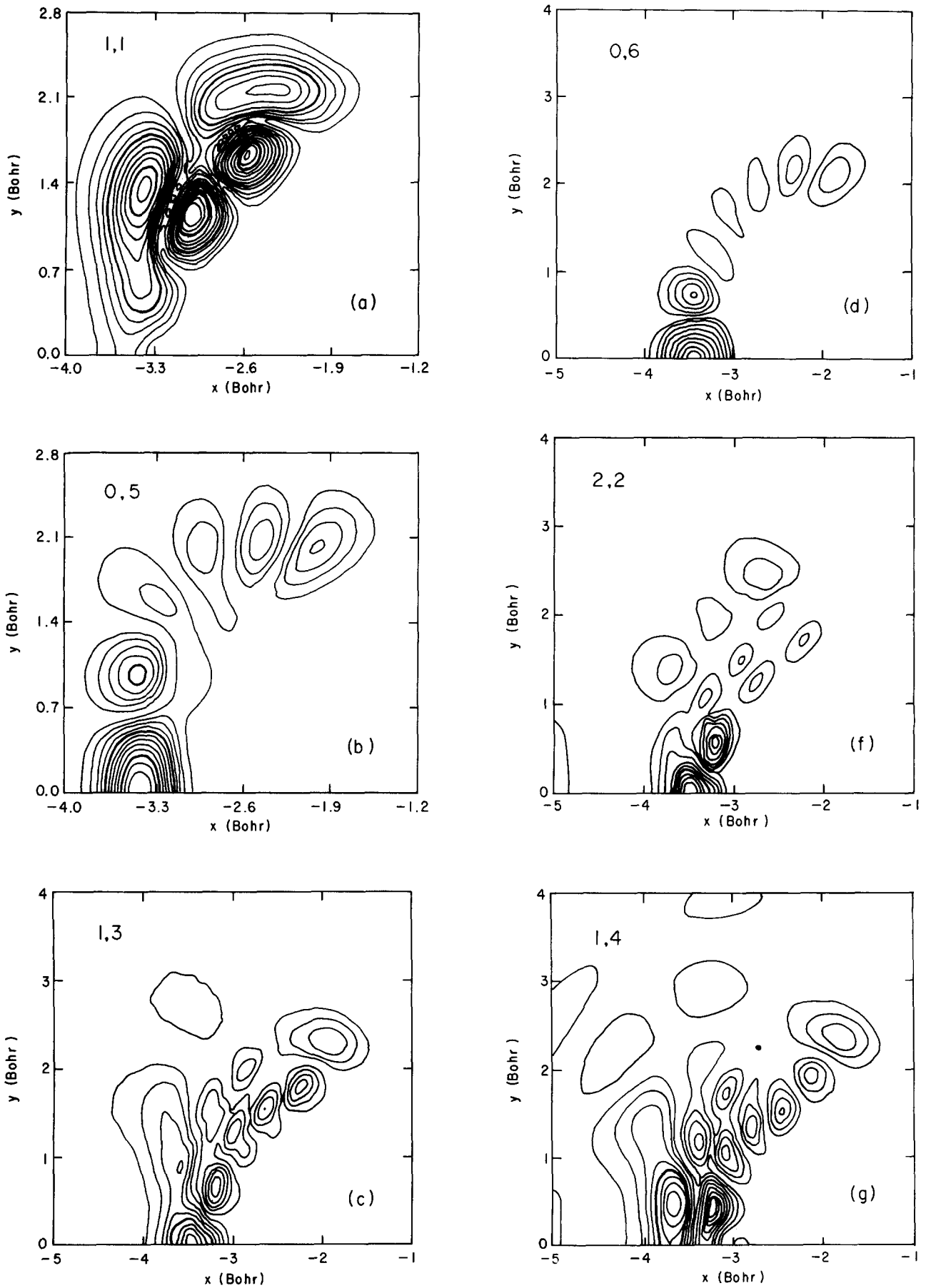


FIG. 4. Quantal (CR) vibrational wave functions for the same states as shown in Fig. 3; the state labels $(v_1,v_2)$ are shown in the upper left-hand corner. Note that there are no Figs. 4(e) or 4(i) since the quantal calculations indicate that the corresponding states, (3,1) and (3,2), are continuum rather than metastable states.

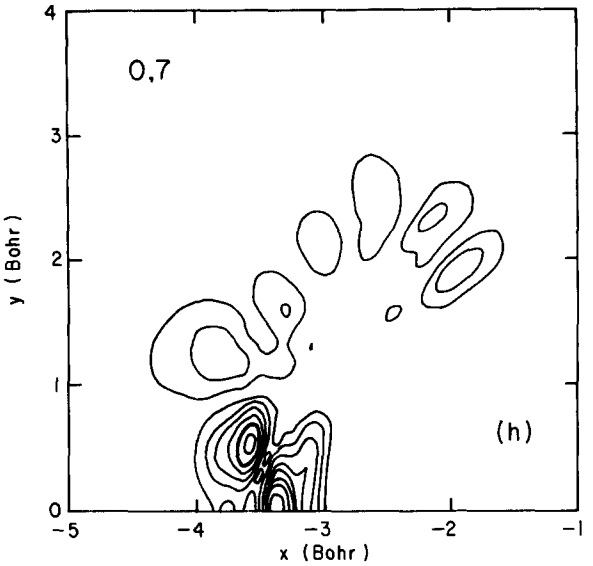


FIG. 4. (*continued.*)

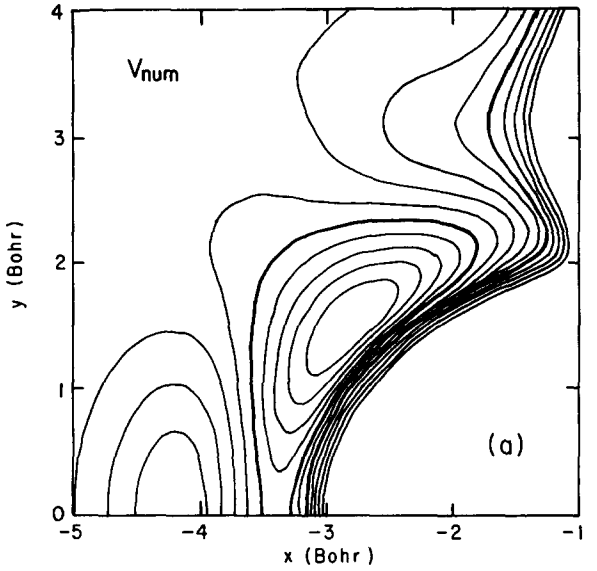


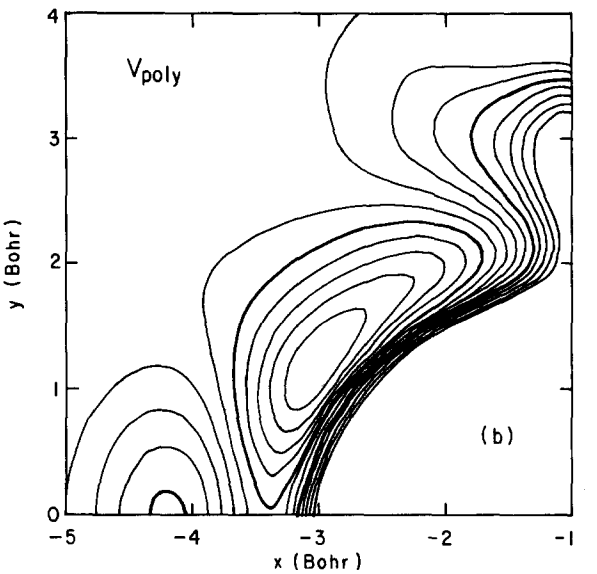


FIG. 5. Comparison of the two functional fits of the potential energy surface. In both plots, the division between contours is 0.0030 hartree. (a) $V_{\text{num}}$ (CR studies); (b) $V_{\text{poly}}$ (SQ studies).

The smaller amount of bulge in the SQ wave functions cannot be due to the surface differences, as the broader escape channel in $V_{\text{poly}}$ would *favor* bulge. This is instead a quantum effect: the semiclassical wave functions do not "know" about tunneling and classical escape, both of which cause bulge.

Upon discovering the surface differences, we attempted to calculate high energy $\psi^{\text{SQ}}_{\text{num}}$ wave functions. However, the surface $V_{\text{num}}$ evidently has a very small fraction of phase space which is regular for higher energies, and we were unable to locate suitable quasiperiodic trajectories at high energy on $V_{\text{num}}$. (The power spectrum Fourier analysis method used in SQ is meaningless unless the trajectory very nearly repeats its motion after closing—that is, it must be quasiperiodic.) Chaotic trajectories do not generally close; due to the exponential propagation of numerical errors in chaotic trajectories, those which do appear to close are not meaningful for SQ. A few saddle-crossing regular trajectories *were* found for $V_{\text{poly}}$, but they did not sample most of the energy-accessible phase space [they looked, e.g., like Fig. 2(f) of Ref. 7.] Such trajectories cannot be used to generate good wave functions for the entire coordinate space.

A more systematic search for regular, high energy trajectories on $V_{\text{num}}$ was made using surface-of-section analysis. The results indicate that short-term quasiperiodic behavior does occur ("vague tori"[22] were found), but that the regular region is exceedingly small—probably vanishingly small above threshold. There have been recent studies which indicate that the amount of energy in the bending mode of a triatomic molecule correlates more closely with the onset of chaotic behavior than does the toal vibrational energy of the triatomic.[23] Our results seem to confirm this, as it is regular trajectories which cross the saddle (bend a lot) which are so difficult to locate.

To close this discussion, we note that the question of how accurate SQ wave functions are for resonance states cannot be definitively answered by these studies, due to the surface differences. This points out one limitation of our version of SQ: appropriate closing trajectories for use in obtaining the power spectrum will be difficult to locate in multidimensional systems with many bending degrees of freedom. Indeed, for such systems, the problem will arise in the study of *bound* states as well as resonances.

### 2. Nonquantization of trajectory action

It is conceivable that in failing to quantize the action of the trajectories we have introduced error. However, previous studies which *did* quantize the action have sometimes yielded SQ wave functions for high energy bound states which were likewise "too regular."[5] Neglecting to quantize the action causes errors in the energy $E_j$, and only secondarily errors in the wave functions [via the phase factor $\exp(iE_j t/\hbar)$]. We do not obtain the energy (position) of the resonance by the usual SQ algorithm,[7–9] however, so not quantizing the action is probably not a significant contributor to errors in $\psi^{\text{SQ}}_{\text{poly}}$.

#### 3. Extrapolation errors

By using bound trajectories, we must necessarily obtain our resonance wave functions from power spectrum peaks which are 100–1000 $cm^{-1}$ above the energy of the propagating trajectory. In paper II, we noted that the further from the energy of the trajectory one extrapolated, the less reliable were the SQ wave functions obtained.[7,24] For the resonance states, we are not only extrapolating to states which sample higher energy regions of the potential energy surface, we are also extrapolating to different kinds of *motion* (from the quasiperiodic regime, to dissociative motion). In this sense, we are forced to extrapolate much further than in the studies of paper II, and this is probably a significant source of error in $\psi^{SQ}_{poly}$.

#### 4. Wave packet spreading and scattering

In the SQ method as implemented here, the wave packet is not allowed to spread or otherwise distort as it propagates along the classical trajectory. This restriction causes no errors for a harmonic potential whose frequency matches that of the packet, but the wave packet would actually spread and distort for our very anharmonic surface (in fact, it is only for a harmonic potential that the wave packet center exactly follows a classical path).[4] Studies which allow the Gaussian packet to distort (but still propagate it along a single classical trajectory) indicate that this improvement is still not adequate for reactive scattering situations.[25] Instead, the wave packet should be allowed to split (scatter) on encountering inflection points of the potential surface, as would a quantally propagated wave packet.[25,26] This is not feasible within the semiclassical formalism used here (but see below).

### B. Changes in SQ required for study of resonances

Since the calculations reported here were completed, a number of workers have suggested variations on the semiclassical wave packet methods. We discuss below those which sound promising for our system, including a few ideas of our own.

#### 1. Expansion to many packets

It has been suggested that one should expand the original wave packet as a sum of wave packets whenever the propagating trajectory encounters pathological (strongly anharmonic or inflection point) regions of the potential energy surface.[25,27] These several wave packets would then be propagated independently (or, as a better approximation, coupled to each other)[27(d)] along their own trajectories, which would tend to diverge with time. If the original trajectory had an energy above threshold, some branches might eventually dissociate. For our problem, this would include coupling to the continuum via the dissociating trajectories. There are two objections to this, however. First, this scheme likely would become computationally intractable, unless one were able to ignore or combine most of the packets at each branch. Second, if slight perturbations of the original trajectory lead to qualitatively different kinds of behavior (i.e., some branches dissociate, others do not), then as discussed by Percival[3(a)] the original trajectory is not really suitable for EBK quantization. We do not have answers to these objections as yet, but by analogy with quantal studies of time-dependent wave packets, this scheme is appealing.

#### 2. Rejection of power spectrum peaks

As noted at the end of Sec. III, the SQ method apparently predicts spurious resonances for the (3,1) and (3,2) states. However, criteria may exist for rejecting certain peaks in the power spectra. One possible criterion is that before associating a power spectrum peak with a resonance state, the peak must appear in the power spectra from several different trajectories sampling the same region of phase space (the trajectories should not resemble each other very closely). De Leon and Heller successfully solved a similar problem in their SQ study[9]; in that case, certain peaks of the power spectrum corresponded to negative quantum numbers.[28] Judicious choice of initial conditions decreased the amplitude of these "ghost peaks"; there may be an analogous way of eliminating the peaks corresponding to our spurious resonances.

#### 3. Semiclassical stabilization

This suggestion stems from a desire to include dissociative and other chaotic trajectories. Quantally, the stabilization method is implemented by systematically changing the basis set in a variational calculation, and associating resonances with those eigenvalues above threshold which are stable with respect to the basis set variation. In a proposed semiclassical stabilization method, one augments the potential surface with an infinite barrier at some value $r_0$, and propagates an essentially arbitrary classical trajectory at an energy above threshold. The barrier reflects the dissociated fragment back into the interaction region, and *eventually* the trajectory closes to some tolerance. One then applies the SQ algorithm of the present paper, and obtains a power spectrum (presumably, the fundamental frequencies of the system will be reflected in the pseudoperiodic motion of the dissociating fragment). The entire procedure is repeated, using a slightly different value of $r_0$ (or, alternatively, slightly changed initial conditions), and the resulting power spectrum is compared with the first one. Any large peaks which occur in *both* spectra (more generally, those which persist for many power spectra) would be candidates for resonances. (These postulated persistent peaks are reminiscent of the "scars" noted by Heller in the wave functions for the stadium billiards problem.[29]) Unfortunately, this may be an untestable conjecture, as the desired trajectories would cover a huge amount of phase space, and have an extremely long closing time. It might be feasible, however, to test this method on the collinear scattering problem, $A + BC \rightarrow AB + C$, by placing a similar barrier in the reactive exit channel.

#### 4. Adiabatic switching

Recently there has been great interest in the fact that, for a sufficiently slowly switched on perturbation, the action variables of a system are conserved.[30–32] One generally starts with a separable system for which the actions are easily calculated, and specifies the initial conditions so that the ac-

tions are the correct EBK values. One then slowly switches on the perturbation, which need not be small; when it is fully "turned on," the actions are still the correct EBK values, and the energy is the EBK energy. This procedure is repeated for various initial conditions, and the results are averaged. It has been discovered by computational experiment that this method can tolerate some chaos.[31] For our DCN problem using $V_{poly}$ as the unperturbed Hamiltonian, and adiabatically switching to $V_{num}$ one should be able to obtain semiclassical estimates for the resonance energies. This might allow rejection of the spurious resonances (3,1) and (3,2). Of course, the unperturbed problem on $V_{poly}$ would be considerably more difficult than the uncoupled oscillator starting point used by Skodje *et al.*[31] Furthermore, this represents a considerable departure from our simple SQ method.

#### 5. Time-dependent variational principle (TDVP)

The SQ method represents a rather specialized evolution of the original wave packet method, which had its inspiration in the Dirac–Frenkel–McLachlan time-dependent variational principle.[33] Since a single frozen wave packet propagated on a classical path does not seem adequate for this problem, it seems appropriate to return to the TDVP and consider using more than one wave packet. Several workers have performed TDVP calculations using multiple packets, with a reasonable effort-to-results ratio.[34,35] There are also possibilities for the single-packet approach, in which the constraint of motion along a classical path is removed; Skodje and Truhlar have explored this possibility.[35] Other workers have suggested one- or few-packet approaches in which the Gaussians are premultiplied by time-dependent polynomial factors, which could better describe a scattered wave packet. These ideas are being pursued in our laboratory and elsewhere.

#### 6. Distributed Gaussian basis sets

Recently, Hamilton and Light[36] constructed a vibrational basis set of real Gaussian functions with their centers distributed uniformly over the energy-accessible coordinate space. These functions were then used in a variational calculation for a two-dimensional vibrational problem. For a polyatomic molecule, the number of functions required would be prohibitively large, unfortunately. Davis and Heller[37] earlier formulated a similar basis set using complex Gaussians (i.e., wave packets) distributed throughout *phase* space, and performed variational calculations. They placed the functions along classical orbits; the resulting eigenfunctions were quite accurate for eigenvalues close to the energy of the classical orbit.

The advantage of placing the functions along a trajectory is, of course, the great reduction in the number of functions required. The trajectory places the Gaussians in the important regions of phase space by its dynamics. (Of course, several trajectories, hence several basis sets, are needed to describe all the dynamics and energetics of the system.) Note that a variational calculation is performed, and the coefficients (i.e., the phases) of the Gaussians are determined by quantum mechanics. The usual semiclassical wave packet approach[4] determines the phases from the trajectory action.

As a hybrid procedure, one can form linear combinations of Gaussian wave packets, determining the relative phase semiclassically by SQ or TDVP, and use these contractions as basis functions in a relatively small variational calculation. This has been done for the bound states of the Henon–Heiles potential, using Gaussians placed along a trajectory and semiclassically contracted in various ways; the results so far are promising.[38] Such an approach can be as quantal or as semiclassical as the system requires; one merely changes the number of functions included or the extent of contraction of the basis. This technique could be used to study the resonances of DCN, e.g., by using as a basis the bound SQ wave functions of paper II supplemented with trajectory-based TDVP-contracted Gaussians outside the potential well, and performing stabilization calculations. Work along these lines is being carried out by this research group and by other workers.[38]

## V. SUMMARY

In conclusion, the SQ method of paper II, while very successful at generating wave functions for the bound states of a highly anharmonic system, does not seem to be appropriate for the study of predissociating states of the same system. While a rigorous quantum/semiclassical comparison has not been made, it appears that this particular version of SQ cannot be applied to our surface at energies above threshold. However, the resonance wave functions generated by this algorithm for a very similar surface are at least qualitatively correct, with the exception of the "spurious resonance" wave functions. Semiclassical wave packet scattering calculations by other workers have successfully reproduced quantal results, and thus we are still optimistic that a method closely related to SQ will prove efficient and accurate in locating and describing nuclear motion resonances in unstable systems such as $C$ state DCN.

## ACKNOWLEDGMENTS

DTC would like to thank Professor E. J. Heller and members of his research group for valuable discussions, and for preliminary communication of results. We would like to thank Hugh Taylor for suggestions and discussions. This research was supported by the National Science Foundation through Grants No. 8206845 and No. 8511307, and through their partial support of the DEC 2060 computer facility. DTC also acknowledges support from the U. S. Army (Grant No. DAAG2984K0086 to JS) and from the donors of the Petroleum Research Fund (Grant No. 12710 AC-6 to JS, administered by the American Chemical Society).

## APPENDIX

Since there is no lifetime information in current formulations of the SQ wave packet method, we have used the slow-channel QCT method of paper I to calculate the resonance widths.[6,18] Briefly, this involves running an ensemble of trajectories whose initial conditions are weighted according to a simple quantal wave function (e.g., one can use the

square of the SQ wave functions to generate the initial condition ensemble). Either quantal or SQ predictions for the positions of the resonances should be used for the trajectory initial energies. One propagates the classical trajectories, notes how long each trajectory survives before dissociating, and then plots the fraction of surviving molecules as a function of time. The resulting curve is then fit by a double exponential,

$$F(t) = C_f \exp(-t/\tau_f) + C_s \exp(-t/\tau_s), \qquad \text{(A1)}$$

where $F(0)$ is normalized to unity. The constant $\tau_f$ is relatively insensitive to $(v_1, v_2)$, and is of the order of one D–CN stretching $(v_1)$ vibrational period. $C_f$ increases with $v_1$ (hence $C_s$ decreases); $\tau_s$ depends on both $v_1$ and $v_2$. The trajectories associated with $\tau_f$ are referred to as "fast channel" trajectories, and we have equated these with an underlying continuum at the energy of the resonance.[18] The "slow-channel" lifetime $\tau_s$ we have associated with the resonance lifetime, and it is these slow channel results that are listed in Table I above.

The above scheme runs into difficulties, however, for continuum states. By associating the slow-channel trajectories with the resonance states, we are requiring that there be *no* slow-channel trajectories in an ensemble of initial conditions corresponding to a continuum state, which may be unrealistic. Any QCT ensemble based on a reasonable, localized zeroth-order estimate of the wave function will most likely "accidentally" include some regions of phase space leading to long-lived (slow-channel) trajectories.

We can state this more quantitatively by postulating the existence of "residual slow-channel trajectories" (RSCTs): at any energy, there may always be a certain number of slow-channel trajectories which have *nothing* to do with resonance behavior (see also Ref.20). We rewrite the slow-channel part of Eq. (A1) as

$$C_s = C_{s,T}(v_1,v_2) + C_{s,R}(E). \qquad \text{(A2)}$$

$C_{s,T}$ corresponds to the slow-channel trajectories which are "true" slow-channel trajectories; it would be zero for values of $(v_1,v_2)$ corresponding to continuum (directly dissociating) states. $C_{s,R}$ corresponds to RSCTs, and in our DCN model system it probably decreases slowly with increasing energy of the system (it also depends somewhat on how one models the initial conditions). For the true resonance states, $C_s$ is typically 0.5 to 1.0, and even a fairly large value of $C_{s,R}$ merely causes Eq. (A1) to overestimate $\tau_s$. For continuum states, however, $C_{s,T}$ is zero, and a nonzero value of $C_{s,R}$ ($\simeq 0.3$, see Table I) leads to the spurious long-lived states (3,1) and (3,2).

The reader may object that the above is not a very satisfying answer: it does not really place the true slow-channel QCT lifetime method on firm theoretical grounds, and it does not tell us how to calculate $C_{s,T}$ (or even predict when $C_{s,R}$ cannot be ignored). These are valid objections, and we no longer feel that the slow-channel QCT method is a defensible way to predict the existence of resonances. However, there is some justification for using this method to calculate approximate relative lifetimes of states known (e.g., from quantal calculations or from experiments) to be narrow resonances.


[1] (a) D. T. Chuljian, J. Ozment, and J. Simons, Int. J. Quantum Chem. Symp. **16**, 435 (1982); (b) R. M. Hedges, Jr., R. T. Skodje, F. Borondo, and W. P. Reinhardt, in *Resonances in Electron–Molecule Scattering, van der Waals Complexes, and Reactive Chemical Dynamics*, edited by D. G. Truhlar (American Chemical Society, Washington, D. C., 1984), p. 323; (c) M. J. Davis and A. F. Wagner, *ibid.*, p. 337; (d) B. A. Waite and W. H. Miller, J. Chem. Phys. **73**, 3713 (1980); (e) R. L. Sundberg and E. J. Heller, *ibid.* **80**, 3680 (1984); (f) W. L. Hase, in *Dynamics of Molecular Collisions, Part B*, edited by W. H. Miller (Plenum, New York, 1976), p. 121; (g) W. L. Hase and R. J. Wolf, in *Potential Energy Surfaces and Dynamics Calculations*, edited by D. G. Truhlar (Plenum, New York, 1981), p. 37, (h) J. W. Brady, J. D. Doll, and D. L. Thompson, *ibid.*, p. 213.

[2] (a) N. C. Blais and D. G. Truhlar, Chem. Phys. Lett. **102**, 120 (1983); G. C. Schatz, *ibid.* **108**, 532 (1984); J. N. L. Connor and W. E. Southall, *ibid.* **108**, 527 (1984); G. C. Schatz, L. M. Hubbard, P. S. Dardi, and W. H. Miller, J. Chem. Phys. **81**, 231 (1984); (b) J. T. Muckerman, *ibid.* **56**, 2997 (1972); M. J. Redmon and R. E. Wyatt, Chem Phys. Lett. **63**, 209 (1979); J. F. McNutt, R. E. Wyatt, and M. J. Redmon, J. Chem. Phys. **81**, 1692 (1984); *ibid.* 1704 (1984); (c) G. C. Schatz, J. M. Bowman, and A. Kupperman, *ibid.* **63**, 674, 685 (1975); (d) R. N. Porter and L. M. Raff, in *Dynamics of Molecular Collisions, Part B*, edited by W. H. Miller (Plenum, New York, 1976), p. 1; (e) G. C. Schatz and H. Elgersma, in *Potential Energy Surfaces and Dynamics Calculations*, edited by D. G. Truhlar (Plenum, New York, 1981), p. 287.

[3] (a) I. C. Percival, Adv. Chem. Phys. **36**, 1 (1977); (b) A. P. Clark, A. S. Dickenson, and D. Richards, *ibid.* **36**, 63 (1977); (c) I. C. Percival and N. Pomphrey, Mol. Phys. **31**, 97 (1976); J. Phys. B **9**, 3131 (1976); (d) D. W. Noid and R. A. Marcus, J. Chem. Phys. **62**, 2119 (1975); *ibid.* **67**, 559 (1977); (e) K. S. Sorbie and N. C. Handy, Mol. Phys. **32**, 1327 (1976); **33**, 1319 (1977); (f) F. G. Gustavson, Astron. J. **71**, 670 (1966); R. B. Shirts and W. P. Reinhardt, in *Quantum Mechanics in Mathematics, Chemistry, and Physics*, edited by K. E. Gustafson and W. P. Reinhardt (Plenum, New York, 1981), p. 277; (g) R. T. Swimm and J. B. Delos, J. Chem. Phys. **71**, 1706 (1979); (h) S. Chapman, B. C. Garrett, and W. H. Miller, *ibid.* **64**, 502 (1976); W. H. Miller, *ibid.* **64**, 2880 (1976).

[4] E. J. Heller, J. Chem. Phys. **62**, 1544 (1975); **75**, 2923 (1981).

[5] N. DeLeon and E. J. Heller, J. Chem. Phys. **78**, 4005 (1983).

[6] D. T. Chuljian, J. Ozment, and J. Simons, J. Chem. Phys. **80**, 176 (1984).

[7] J. Ozment, D. T. Chuljian, and J. Simons, J. Chem. Phys. **82**, 4199 (1985).

[8] M. T. MacPherson and J. P. Simons, J. Chem. Soc. Faraday Trans. 2 **74**, 1965 (1978).

[9] N. De Leon and E. J. Heller, J. Chem. Phys. **81**, 5957 (1984).

[10] In SQ as originally proposed, and in the results reported here, the trajectory is chosen from the regular rather than the chaotic region of phase space. Further, in the SQ method of De Leon and Heller, the classical action of the trajectory is required to be quantized (see Ref. 9), but in Ref. 7 it was noted that this does not seem to be necessary.

[11] M. F. Herman and E. Kluk, Chem. Phys. **91**, 27 (1984).

[12] A word of caution: in the power spectrum, peaks corresponding to metastable states are *not* broadened, as they would be, for example, in an absorption spectrum. This is because the SQ method is based on localized, closed trajectories, and in effect assumes that the metastable states are still bound.

[13] W. P. Reinhardt, Annu. Rev. Phys. Chem. **33**, 223 (1982).

[14] B. R. Junker, Adv. Atom. Mol. Phys. **18**, 207 (1982); B. Simon, Ann. Math. **97**, 247 (1973).

[15] Due to the use of contracted bending vibrational functions $x_{v_2}$ (see Ref. 6), the scattering eigenvalues of the rotated Hamiltonian $H_\eta$ correspond to linear combinations of the true scattering states (i.e., the final state of the CN fragment is not a pure rotational state). This means that the metastable states couple to mixed continuum states (i.e., to linear combinations of states with the CN fragment possessing different amounts of angular momentum). This could cause errors in the widths, and to some extent the positions, of the broader resonances, which are more strongly coupled to the continuum.

[16] These results differ somewhat from the values previously reported in Ref. 6. After publication, we developed better computer routines for displaying the wave functions, and discovered that in Ref. 6 we had incorrectly assigned some of the resonances. The results given here also reflect some additional calculations giving better estimates for the positions and widths.

[17] B. R. Junker and C. L. Huang, Phys. Rev. A**18**, 313 (1978); T. N. Rescigno, C. W. McCurdy, and A. E. Orel, *ibid.* **17**, 1931 (1978).

[18]D. T. Chuljian, Ph. D. thesis, University of Utah 1984, Chaps. 8 and 9.
[19]N. Moiseyev, T. Maniv, R. Elber, and R. B. Gerber, Mol. Phys. **55**, 1369 (1985).
[20]S. D. Bosanac, Phys. Rev. A **32**, 871 (1985).
[21]D. T. Chuljian and J. Simons, J. Am. Chem. Soc. **104**, 646 (1982); D. T. Chuljian, Ph. D. thesis, University of Utah 1984, Chap. 4.
[22]R. B. Shirts and W. P. Reinhardt, J. Chem. Phys. **77**, 5204 (1982).
[23]J. Tennyson and S. C. Farantos, Chem. Phys. **93**, 237 (1985).
[24]The maximum energy which one can safely extrapolate above the trajectory energy is dependent on the region of the potential surface being sampled. For wave functions with large amplitude in rapidly changing regions of the potential surface, one must locate a trajectory as nearly isoenergetic with the desired vibrational state as possible.
[25]Ch. Zuhrt, Mol. Phys. **51**, 241 (1984).
[26]C. Leforestier, Chem. Phys. **87**, 241 (1984).
[27](a) E. J. Heller, Chem. Phys. Lett. **34**, 321 (1975); (b) S. Y. Lee and E. J. Heller, J. Chem. Phys. **76**, 3035 (1982). (c) G. Drolshagen and R. Vollmer, Chem. Phys. Lett. **122**, 333 (1985) and Refs. 1 and 2 therein; (d) S.-I. Sawada, R. Heather, B. Jackson, and H. Metiu, J. Chem. Phys. **83**, 3009 (1985).
[28]In Ref. 9, it was also suggested that the problem of "ghost" peaks would decrease as the density of states increased (which usually occurs at high energies). Our surface does *not* show such an increasing density of states (at least, not at the energies studied here), which may be partially responsible for the persistence of the apparently spurious (3,1) and (3,2) SQ resonances.
[29]E. J. Heller, Phys. Rev. Lett. **53**, 1515 (1984).
[30]E. A. Solov'ev, Sov. Phys. JETP **48**, 635 (1978); T. P. Grozdanov and E. A. Solov'ev, J. Phys. B **15**, 1195 (1982).
[31]R. T. Skodje, F. Borondo, and W. P. Reinhardt, J. Chem. Phys. **82**, 4611 (1985).
[32]T. P. Grozdanov, S. Saini, and H. S. Taylor, Phys. Rev. A **33**, 55 (1986).
[33]E. J. Heller, J. Chem. Phys. **64**, 63 (1976).
[34]R. Brown, Ph. D. thesis, University of California at Los Angeles 1983, Chap. 3.
[35]R. T. Skodje and D. G. Truhlar, J. Chem. Phys. **80**, 3123 (1984).
[36]I. P. Hamilton and J. C. Light, J. Chem. Phys. **84**, 306 (1986).
[37]M. J. Davis and E. J. Heller, J. Chem. Phys. **71**, 3383 (1979).
[38]J. Ozment and E. J. Heller, J. Chem. Phys. (submitted).